Video Article

Near-infrared Navigation System for Real-time Visualization of Blood Flow in Vascular Grafts

Srikar Raman*[1], Sarah Hansen*[2], Charles Jr. Caldwell[3], Vaishnavi Raman[1], Henry White[1], Craig Emter[4], Ajit Tharakan[5], Anandhi Upendran[6,7], Raghuraman Kannan[1,3]

[1]Department of Radiology, University of Missouri

[2]Office of Animal Resources, University of Missouri

[3]Bioengineering, University of Missouri

[4]Biomedical Science, University of Missouri

[5]Surgery - Division of Cardiothoracic Surgery, University of Missouri

[6]MU-iCATS, University of Missouri

[7]Medical Pharmacology and Physiology, University of Missouri

*These authors contributed equally

Correspondence to: Raghuraman Kannan at kannanr@health.missouri.edu

Abstract

Vascular grafting failures are often attributed to inadequate anastomotic perfusion assessments. If successful, vascular anastomosis can be rapidly confirmed through the visualization of continuous blood flow upon completion of the grafting process. Surgeons can then minimize graft failures, thus decreasing morbidity in a cost-effective manner. Fluorescence image-guided surgery using near-infrared (NIR) dye is one of the methods that can be performed to monitor grafting success. To address the current logistical challenges and costs of these systems, a compact camera system was used for intraoperative fluorescence real-time NIR imaging. Combined with benchtop experiments, a swine model was used to demonstrate the procedure of using a near-infrared navigation system (NAVI) to visualize grafted vessels *in vivo*. This was done by performing bilateral arteriovenous grafts and imaging intravenously injected ICG as it circulated through the grafted vessels. The fluorescent images obtained by NAVI were corroborated with Doppler flow measurements and cine-angiography, the current gold standard for the evaluation of vascular grafts.

Introduction

Intraoperative assessments of blood flow following arterial or venous grafting, as well as direct visualization methods evaluating anastomosis, allow surgeons to make immediate decisions on the likelihood of success or failure, allowing for repair, if needed[1,2]. Techniques frequently employed are fluoroscopic angiography[3], direct visualization, palpation of pulsatile flow, pulse oximetry[2], Doppler ultrasound[4], transit time flowmetry[5,6,7], computed tomography angiography[8], and visible light and near-infrared spectrophotometry[9]. As the evaluation of surgical outcomes continues, improvements in equipment and an increasing availability of technology allow for the more widespread use of these methods. Challenges exist in many of these techniques; while they are excellent at evaluation, some limitations include cumbersome equipment, a lack of proper anatomical definition, and exposure to radiation[10]. One technique that avoids many of these drawbacks and that has been tested across a wide variety of surgical repairs is the use of near-infrared (NIR) fluorescence imaging, specifically with FDA-approved indocyanine green (ICG)[11]. ICG fluoresces brightly at low concentrations and is well confined to the vasculature due to its high plasma protein binding capabilities[12]. Additionally, the liver clears it from blood circulation within minutes, allowing for multiple injections[13,14].

Fluorescence image-guided surgery is an optical imaging procedure that allows surgeons to visualize real-time tissue images and to evaluate circulation and perfusion intraoperatively. Capturing real-time images improves surgical outcomes by allowing the rapid identification and repair of graft failures[15]. ICG is injected intravenously and visualized under an NIR wavelength range (700-900 nm). ICG visualization in this wavelength range results in high contrast against a black background due to minimal tissue absorbance and scattering, meaning minimal auto-fluorescence. While frequently used to measure hepatic function and ophthalmic angiography[11], this dye has shown promise for several procedures that include but are not limited to: lymphatic mapping[16,17,18,19], hepatobiliary surgery[20], dermal vasculature mapping for burn wound severity[21], cerebral aneurysm repair[22,23], gastrointestinal anastomosis verification[24], and venous and arterial grafting[12]. A recent, encompassing review of the usage of ICG in surgical procedures revealed the need for improvements in the image processing, portability of the instrumentation, and economic viability[12].

A portable and economical fluorescence imaging system that could serve as an alternative to the costly and unwieldy existing fluorescence imaging modality is desired to assist surgeons in intraoperatively evaluating the success of the vascular grafting process. We used a portable NIR navigation system (NAVI), which has the capability of visualizing ICG in deep tissues and recording real-time images with high sensitivity.

The ability of the NAVI system to visualize selected regions of interest, confirm blood flow, and detect leaks from sites of anastomosis has been demonstrated by *in vivo* arteriovenous grafting procedures in a swine study.

The integral components and assembly of NAVI (**Figure 1**) for the visualization of florescence emitted from ICG are listed and briefly described below. The source is five 770-nm NIR LEDs assembled onto a battery DC power supply, with a 775-nm short pass filter. The short pass filter allows only 770-nm emitted light to reach the imaging site while reducing any possible stray radiation above 770 nm. The camera is an NIR imaging camera with an added band pass filter. The width of the pass region is 37 nm, centered at 832 nm, and is employed for the purpose of rejecting radiation collected by the NIR imaging camera that does not emanate from ICG fluorescence or from stray light. The NIR imaging camera has an RCA analog output for the image signal. The interface is the composite video image from an NIR imaging camera that is interfaced to a USB port on a computer via an analog-to-video interface designed to translate composite video to digital for the purpose of capturing, storing, processing, and providing the output of the digital signal to an image display unit. The interface system accepts the analog output. The computer is a single-board with a USB input that has the processing capabilities necessary to store and process images. The monitor is a conventional video monitor of any size and is used to display the images generated by the computer. The stands are two mechanical arms for suspending the source and NIR camera over selected tissue areas, as well as a foot control that aids in the movement of the NIR camera.

Protocol

Animal studies were performed following approval from the University of Missouri Animal Care and Use Committee. The University of Missouri is USDA-licensed and AAALAC-International accredited.

1. Pre-operation procedure

1. Obtain a domestic Yorkshire/large white pig (4 months old; 57 kg) one day prior to the study and provide water *ad libitum*.
2. Sedate the pig with 5 mg/kg Telazol and 2.2 mg/kg xylazine. Provide 3-4% isoflurane by nose cone until the pig can be intubated and then reduce the isoflurane to 2%.
3. Intubate the pig, attach ECG leads, and place the pig on mechanical ventilation for the entire procedure. Confirm the depth of anesthesia by performing a toe pinch and observing the loss of the pedal reflex. Throughout the procedure, monitor the heart rate, absence of limb withdrawal, and absence of palpebral reflex to ensure the maintenance of a surgical plane of anesthesia.
4. Place the pig in dorsal recumbent position on the operating table.
5. Place a 20-gauge IV catheter in the right auricular vein. Administer IV fluids (0.9% NaCl) at 5 mL/kg/h via an auricular catheter.

2. Carotid artery grafting

1. Incise approximately 12 cm of the jugular furrow with a size-10 scalpel blade. Expose the external jugular vein and the carotid arteries via blunt dissection of the sternomastoidius and sternocephalic musculature using Metzenbaum scissors.
2. Using curved Metzenbaum scissors and Adson-Brown tissue forceps, dissect an 8-cm segment of the right jugular vein. Apply proximal and distal 2-0 silk ligatures and remove it.
3. Apply vascular clamps to the carotid artery and make a small, vertical arteriotomy on the anterior wall of the vessel. Circumferentially suture one end of the jugular vein with 6-0 Prolene sutures to the arteriotomy in an end-to-side manner to complete the proximal anastomosis.
4. Likewise, perform distal anastomosis with the other end of the jugular vein to complete the graft.
5. Remove the clamps to allow the diverted blood to flow through the graft.
6. Repeat the jugular vein grafting on the contralateral side.

3. Visualization by NAVI

1. Prepare 10 mL of ICG (1 mg/mL) solution in sterile water in a sterile red-top tube and keep it protected from light. Draw up the injection amount with a sterile 20-gauge needle and syringe, as needed.
2. Focus the camera, adjust the NIR light source, and open the software preloaded in the laptop screen. Use low ambient light and turn off all room lights when the camera is functioning.
3. Rapidly inject 3.0 mL of ICG (0.05 mg/kg) in the auricular catheter and flush with 8 mL of sterile saline.
4. After the injection of ICG, press the small switch on the NIR light source to turn it on and illuminate the graft region; simultaneously press the switch to turn on the NIR imaging camera.
5. View the fluorescent images on the laptop screen. Simultaneously, click the record icon in the software to record the images.
6. Wait approximately 7 min to allow the fluorescence of the ICG to diminish.
7. Place vascular clamps in the middle of the graft to occlude anastomosis. Repeat the injection at a lower dose of 1.5 mL of ICG (0.03 mg/kg) and flush with saline.
8. Repeat steps 3.2-3.5 to record the flow of ICG into the carotid segment grafting and perform fluorescence measurements on the contralateral side.
9. Perform blood flow measurements simultaneously using Doppler flow probes, as described below in step 4.

4. Doppler probe measurement

1. Use two 3.0-mm Doppler blood flow probes. Place one flow probe onto the carotid artery, cranial to the graft site, and apply ultrasound gel over the probe. After vascular placement, connect the flow probe to the perivascular flow module. Connect the perivascular flow module to an analog-to-digital board, which allows the Doppler signal to be measured as the blood flow in real time using data acquisition software.

2. Place the second flow probe on the bypassed segment of the carotid artery and apply ultrasound gel over the probe. After vascular placement, connect the flow probe to the perivascular flow module. Connect the perivascular flow module to an analog-to-digital board that allows the Doppler signal to be measured as blood flow in real time using data acquisition software.
3. Allow both probes to remain on the vessels for several minutes and record and compare the flow between the two flow probes.

5. Cineangiography procedure

1. Turn on the fluoroscopy unit.
2. Create a medial longitudinal skin incision in the region between the left gracilis and sartorius musculature to access the left femoral artery. Bluntly dissect with curved Metzenbaum scissors and Adson-Brown tissue forceps until the femoral artery is identified.
    1. After placing self-retaining tissue retractors, securely occlude the distal aspect of the femoral artery with 2-0 silk suture and insert a guiding catheter into the femoral artery. Pass the guide wire into the aorta via the femoral artery and external iliac artery.

3. Give a loading dose of heparin (300 U/kg) IV and continue hourly at 100 U/kg.
4. Using a 0.035 mm-diameter flexible guide wire, feed the catheter to the desired location in the carotid artery by way of the brachiocephalic trunk. Remove the guidewire.
5. Inject 8-10 mL of iohexol solution into the carotid artery (visualize each side individually).
6. Press the start key on the fluoroscopy unit to record the images.
7. View the images on a computer loaded with software for viewing the images.
8. Repeat iohexol and image acquisition for the contralateral side by moving the catheter into the contralateral carotid artery.
9. Following these procedures, sacrifice the pig with an IV pentobarbital overdose while under anesthesia.

Representative Results

Optimization of the Concentration of ICG

The concentration of ICG required to produce optimal fluorescent images was determined using the following procedure. Different concentrations of ICG solutions ranging from 1.29 to 258 µM were prepared in microcentrifuge tubes and placed on a stand. The NIR light source and the camera were placed at a constant distance from the dye (*i.e.,* 18 and 31 in, respectively, from the stand). The fluorescent images were recorded using NAVI at all prepared concentrations (**Figure 2**). Fluorescence intensity was minimal at the lowest concentration (1.29 µM). It started to increase at 6.5 µM, and it reached maximum saturation at ~65 µM. Upon increasing the concentration beyond 65 µM, the fluorescence intensity decreased (**Figure 3**) due to the self-quenching fluorescence property of ICG. Therefore, it was concluded that the working concentration range of ICG for NAVI at these distances was in the range of 6.5 of 65 µM.

Optimizing the Distance of the NIR Source and Camera from the Dye

Once the working concentration range of ICG was established, the following experiments were performed to determine the distances of the NIR light source and the camera from the dye. (i) First, the distance between the ICG dye and the NIR light source was optimized. The NAVI was fixed at a distance of 31 in from the ICG microcentrifuge tubes. The NIR light source was placed at varying distances from the ICG. The working range for the distance between the NIR light source and the ICG dye was optimized as 13 to 26 in, optimally at 18 in. Images were recorded and are presented in **Table 1**. (ii) The second step was to determine the optimal distance between the ICG dye and the camera. The optimal distance was identified by fixing the NIR light source at a distance of 18 in from the ICG microcentrifuge tubes. The distance of the NAVI camera from the ICG dye was varied over a wide range-up to 12 ft. Further distances were not explored. The distance between the NAVI and the ICG was altered, and images were recorded (**Table 2**).

Fluorescence Imaging of ICG in the Presence of Human Serum Albumin (HSA)

HSA is an abundant protein in blood; therefore, any interference with ICG may result in a change in fluorescence. Thus, additional experiments were conducted to investigate the interference of HSA on ICG fluorescence. HSA and ICG were mixed in 1:1 and 2:1 molar ratios (2 mL each; ICG concentration: 13 µM). The microcentrifuge tubes containing these two mixtures, along with ICG alone as a control, were placed on a stand. The NIR light source and camera were positioned at distances of 18 and 30 in, respectively, as optimized from the previous experiment, and images were recorded at different time points (6, 12, and 15 min). There was no difference in fluorescence intensities between the HSA and ICG mixed solutions and ICG alone. Therefore, the ratio of HSA:ICG was increased to 4:1 and the fluorescence was observed at different time points. Solutions of HSA:ICG were mixed at a 1:1 volume ratio, added to the microcentrifuge tube, and placed on the stand. No change was observed in fluorescence intensity for any of the tubes, even after 15 min, suggesting that the fluorescence intensity does not decrease within the time frame required to visualize the graft. However, one week later, the fluorescence intensities of HSA-mixed ICG solutions were found to be decreased compared to that of ICG alone, indicating that ICG binds with has, as reported in the literature[12,25,26].

Fluorescence Imaging in a Rabbit

An exploratory study was conducted in a rabbit cadaver immediately following euthanasia to check the image visualization capability of NAVI using optimized parameters. For this purpose, an ICG solution (13 µM) in water was injected intravenously into the ear veins of a rabbit and images were recorded. Immediately after injection, the ICG distributed within the veins, and the fluorescence localized within the ear vein could be detected by viewing it through the skin (**Figure 4**). This study demonstrated that veins in humans up to 4 mm below the surface of the skin can be imaged using the NAVI system.

Fluorescence Imaging using NAVI

After the optimization of all parameters, grafting studies and real-time visualization of blood flow in carotid artery grafts were conducted by performing fluorescent imaging using the NAVI system. The carotid artery grafting was successfully completed (**Figure 5**) on one side, and ICG was initially injected at a dose pf 0.05 mg/kg to monitor the fluorescence. The NAVI system was connected to a monitor to capture the images. The flow of ICG through the carotid artery and jugular vein graft through 500-600 cardiac cycles was observed (the average heart rate throughout was 80 bpm). After 7 min, a decrease in fluorescence intensity was observed. The focusing parameters of the camera and NIR lights were altered slightly, and ICG was injected at a dose 58% lower (0.03 mg/kg) to obtain high-resolution images. When vascular clamps were placed to occlude the flow through the graft, there was interruption in the flow of ICG. However, the flow remained continuous in the native carotid segment. When the clamps were released, the flow resumed into the venous graft. Fluorescent images recorded during and after the clamp release confirmed the observation. For the contralateral side, 0.03 mg/kg ICG was injected. Fluorescent images were recorded to again monitor the flow of ICG over 7 min, or approximately 500-600 cardiac cycles. Due to the disparity in size of the donor vein relative to the carotid artery disrupting laminar flow, swirling of the blood was observed in the graft, while the carotid flow was continuous. Vascular clamps were applied and fluorescent images were recorded before and after applying the clamps. Doppler flow measurements were concurrently performed.

Carotid and Graft Transonic Flow Measurement

Fluorescent imaging of ICG was compared to other standard techniques that are currently in clinical practice. In swine experiments, two Doppler blood flow probes are placed at separate locations on the carotid artery: one between the proximal and distal carotid access points of the jugular graft (location #1), and one distal to the exit of the of the carotid anastomosis (location #2) (**Figure 6, and Figure 7A**). **Figure 7B** demonstrates the validation of changes in the ICG fluorescence signal through the anastomosis and carotid. When the anastomosis was open, carotid blood flow on Channel 1 (location #1) was decreased beyond the total carotid blood flow, as assessed on Channel 2 (location # 2), and was associated with high fluorescence in the jugular graft. When the anastomosis was occluded, the carotid blood flow increased at location #1, making it equal to that at location #2, and was associated with a reduction in fluorescence in the jugular graft and a commensurate increase in the carotid artery. Carotid blood flow was again reduced upon the reopening of the anastomosis at location #1. The procedure was repeated for the contralateral side, and similar results were obtained.

Cineangiography

Blood flow through the grafts was further confirmed via cineangiography. When the catheter was passed into the origin of the carotid artery, iodixanol was injected and could be visualized as it passed through the grafted vessels. When the graft was occluded with forceps and the injection was repeated, iodixanol was visualized throughout the native vessel. This procedure was repeated on the contralateral side.


Figure 1. Picture of the near-infrared navigation system
The NAVI consists of five NIR LEDs with a short band pass filter, which acts as light source to excite the region of interest, and a camera with an added band pass filter.
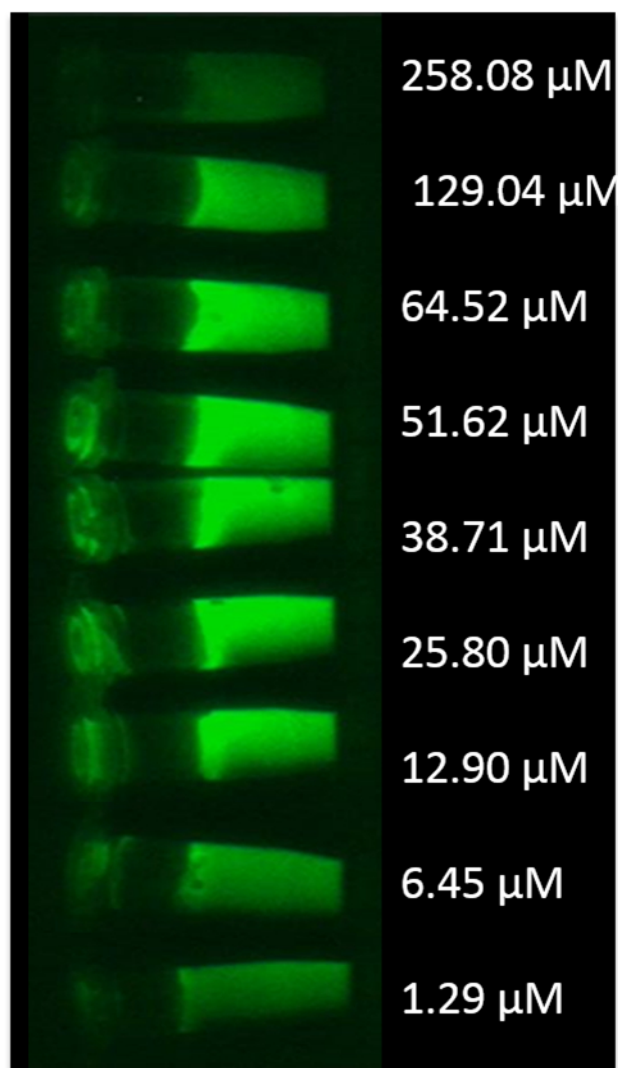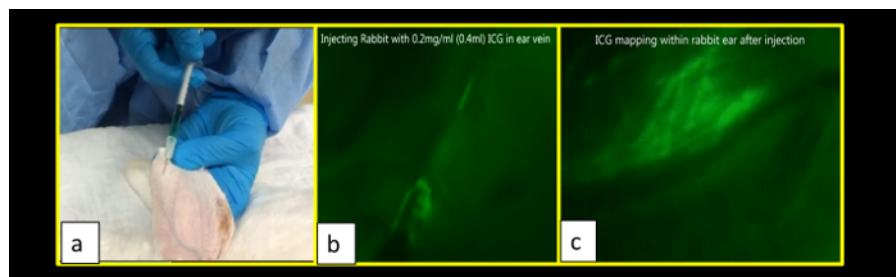
Figure 2. Fluorescent images of ICG solutions at different concentrations
The NIR light source and the camera were placed at constant distances from the dye (*i.e.,* 18 and at 31 in, respectively, from the stand), and fluorescent images were recorded using NAVI at concentrations ranging from 1.29 to 258.08 µM.
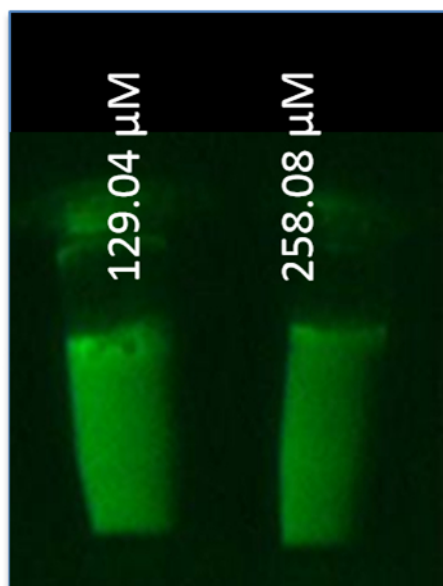
Figure 3. Fluorescent images of ICG solutions above the concentration of 65 μM
The NIR light source and the camera were placed at constant distances from the dye (*i.e.,* 18 and at 31 in, respectively, from the stand), and images were recorded using the NAVI. Upon increasing the concentration beyond 65 μM, the fluorescence intensity decreases due to the self-quenching fluorescence property of ICG.


Figure 4. Fluorescent images of rabbit ear vein
Fluorescent images of a rabbit ear vein were recorded using the NAVI following an ICG injection. (a) ICG solution (13 μM) was injected into the ear of a rabbit following euthanasia prior to imaging. (b) Immediately after the injection, the ICG distributed throughout the ear vein, and fluorescent images were recorded using the NAVI. (c) Upon completion of the injection, the ICG distributed throughout the veins, and the fluorescence localized within the ear vein could be detected by viewing through the skin of the rabbit. Please click here to view a larger version of this figure.
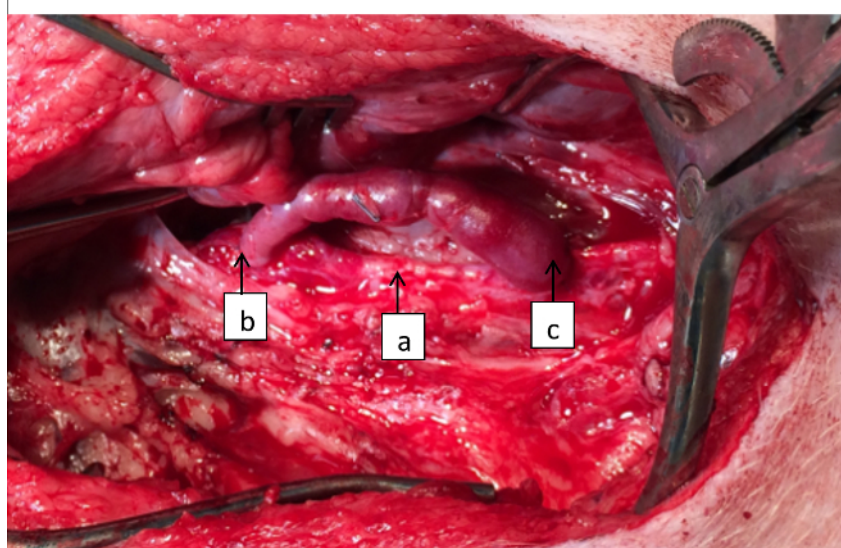
Figure 5. Left-side vein grafting procedure image
Image of the left side of the surgical field upon completion of the grafting procedure. The left jugular vein served as the graft, and the left carotid artery served as the native vessel. (a) The native carotid artery. (b) The proximal end of the graft. (c) The distal end of the graft. The graft demonstrates no obvious leaks at the anastomotic sites. Please click here to view a larger version of this figure.
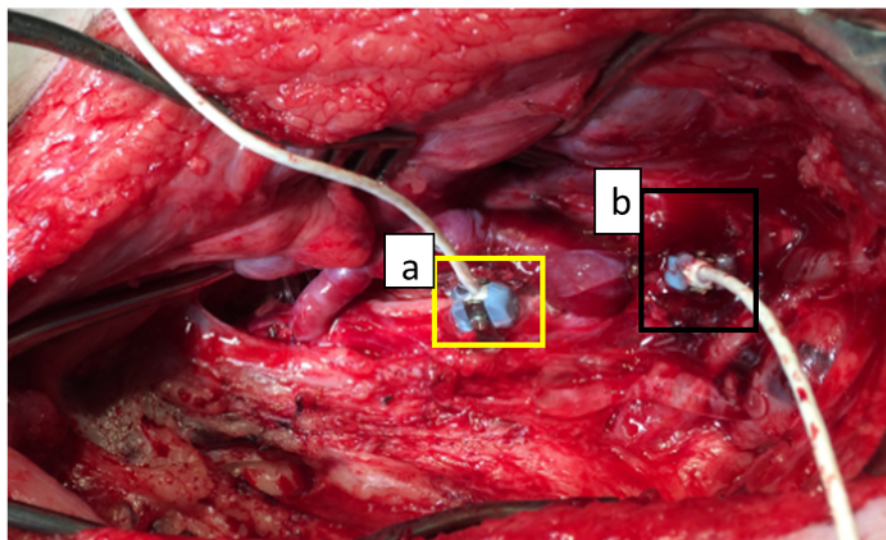

Figure 6. Doppler blood flow measurements
Doppler flow probes placed at two locations on the carotid artery for Doppler measurements. (A) The yellow box shows the probe placed on the native carotid vessel, between the proximal and the distal anastomotic sites. (B) The black box shows the second probe, distal to the distal anastomotic site on the carotid artery. Please click here to view a larger version of this figure.
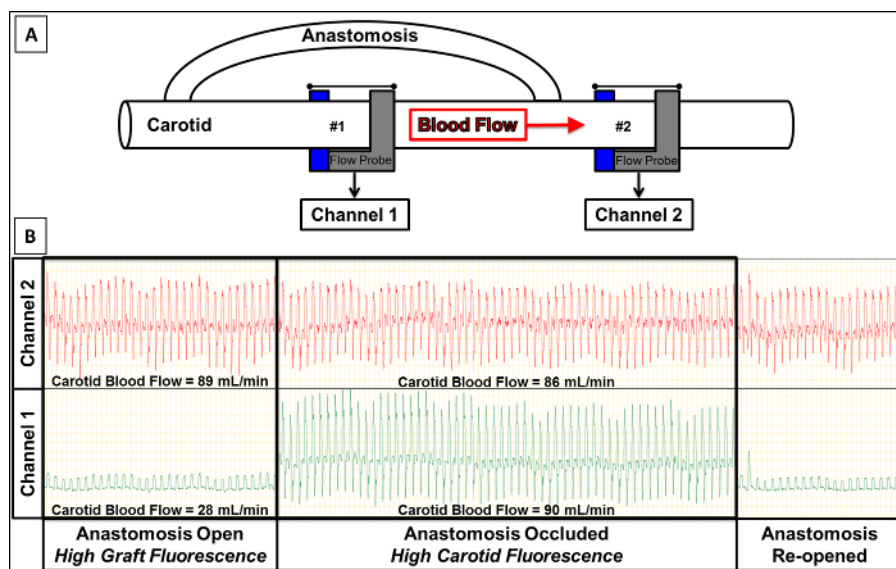
Figure 7. Schematic representation of blood flow measurements using Doppler flow probes
Blood flow through the graft and the carotid was measured using Doppler flow probes. (a) The placement of the flow probes at location #1 (between the proximal and distal carotid access points of the jugular graft) and location #2 (distal to the exit of the of the carotid anastomosis). (b) Graphical demonstration that when the anastomosis was open, carotid blood flow on Channel 1 (location #1) was decreased beyond the total carotid blood flow, as assessed on Channel 2 (location # 2). When the anastomosis was occluded, carotid blood flow increased at location #1, making it equal to that at location #2. Please click here to view a larger version of this figure.
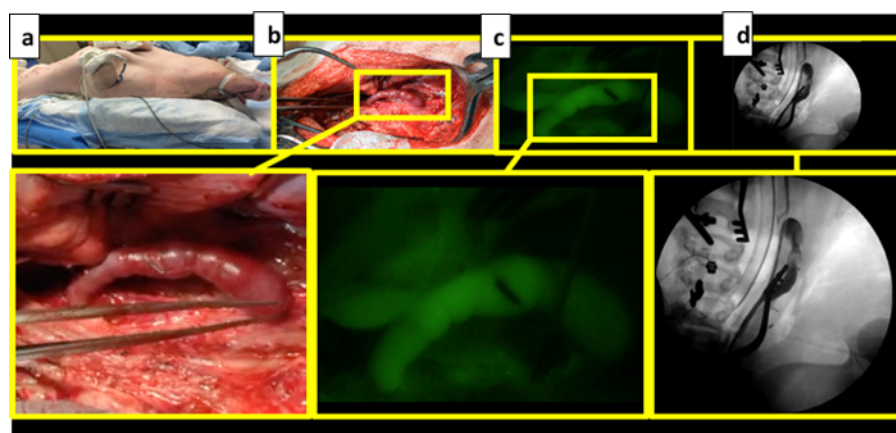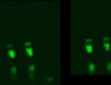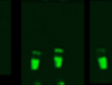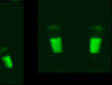

Figure 8. Comparative vein grafting images
Gross images and those obtained with the NAVI and by angiography procedures are shown for comparison. (a) Swine in dorsal recumbent position. (b) Gross section following a vein grafting procedure. (c) Fluorescent image of the graft obtained following the injection of ICG. (d) Standard angiography CT image obtained following the injection of iohexol (contrast agent). Please click here to view a larger version of this figure.

Distance (inches)	62	50	38	26	20	18	13	7
NAVI Fluorescent Images								

Table 1. Change in fluorescence upon varying the distance between the NIR source and the ICG dye at two different concentrations: 12.90 µM (left) and 25.80 µM (right). Please click here to view a larger version of this figure.

Distance (inches)	144	124	96	72	60	48	41	31
NAVI Fluorescent Images								

Table 2. Change in fluorescence upon varying the distance between the camera and the ICG dye at two different concentrations: 12.90 µM (left) and 25.80 µM (right). Please click here to view a larger version of this figure.

Discussion

Development of NAVI for ICG Imaging Applications

NIR-based fluorescence imaging is emerging as a simple alternative procedure for intraoperative imaging, demonstrating significant benefits by: (1) eliminating the radiation exposure required by fluoroscopy and computed tomography and (2) reducing the surgical time, thus decreasing per-patient costs while maintaining efficacy and increasing safety. In this paper, we demonstrated the procedure for using NAVI to perform fluorescence imaging (using ICG dye) in a large-animal model. The development of this compact, user-friendly system included the optimization of the NIR light source placement and the camera distance from the field of view. The working concentration ranges were also optimized by using a range of solutions to characterize the operation and sensitivity of the of NAVI before animal studies were conducted. ICG shows an absorption maximum at 805 nm and emission maximum at 830 nm in plasma. The NAVI utilizes five 770-nm NIR LEDs along with a 775-nm short pass filter. The short pass filter allows 770-nm radiation to reach the imaging site while reducing any possible stray LED radiation above 770 wavelengths. The NAVI is coupled with an NIR imaging camera with band pass filter. The width of the pass region is 37 nm, centered at 832 nm, and is used to reject radiation collected by the NIR imaging camera that does not emanate from ICG fluorescence or from stray light. *In vitro* and cadaver studies were used to optimize the required distances and the field-of-focus ability prior to proceeding to *in vivo* testing.

Based on the preliminary *in vitro* and cadaver studies, in order to observe the fluorescence and to confirm the success of vein grafting, it is critical to place the NIR light source at an angle of 45° and 30 cm directly above the graft or the region of interest. The imaging camera should be placed perpendicularly to the graft at a distance of 70 cm to obtain fluorescent images. The flow of ICG through the graft is very quick and, to capture images, the camera and light source should be set for operation prior to injecting the ICG.

ICG Dosage Variation Between *In Vitro* and *In Vivo* Studies

ICG dose is also a critical parameter, as the fluorescence is only observable at a certain range of concentrations. *In vitro* studies performed earlier in device development utilized a low concentration range. However, it is important to note that the dilution factors in the circulating blood volume were not required; thus, a higher concentration would be required to monitor fluorescence *in vivo*.

Initially, a slightly higher dose than the one that is reported in the literature for the purpose of imaging ICG in pigs was used. Detter *et al*. reported 0.03 mg/kg in 2002[27] and 2007[1] (into the central venous line), while *Tanaka et al*. reported using 0.06 mg/kg in 2009[28]. After the completion of left-side grafting, ICG was injected at a dose of 0.05 mg/kg and fluorescent images were recorded. When ICG was used at this dose, fluorescence was observed, but the camera gain had to be lowered and the focus had to be adjusted due to high saturation in the images. The imaging was performed for 7 min when the fluorescence diminished completely. It appeared that fluorescent images could be obtained at a lower dose and therefore, the ICG dosing was reduced to one-half (0.03 mg/kg). When the dosage of ICG was decreased to one-half, the fluorescent images and the blood flow visualization demonstrated a dramatic improvement due to the optimal fluorescent intensity. Even though the dose of ICG was decreased, the timeframe of observed fluorescence remained the same (7 min). For all subsequent injections, a dosage of 0.03 mg/kg was used and the fluorescence was found to be acceptable.

Although pig models are frequently used to evaluate human cardiac disease, the use of ICG in pigs for modeling other surgical interventions requires further dosage optimization. For example, a 2016 human study by Zarrinpar *et al*. reported the improved visualization of biliary structures in patients when the ICG dosage was increased from 0.02 mg/kg to 0.25 mg/kg, as well as an improvement after allowing increased time to pass following the dosage (45 min was superior to 10 min)[20]. As ICG imaging becomes more mainstream, the optimization of dosage and timeframe for each particular usage will likely be reported.

***In Vivo* Testing Verifies the Functionality and Ease of Use of NAVI**

Jugular vein to carotid artery grafting modeling human arteriovenous grafting was completed bilaterally in a large-animal model. ICG was administered via a peripheral intravenous catheter after the completion of anastomosis to monitor the grafting success. Within minutes of injection, the dye was visualized to circulate through the grafted vessel and carotid artery. The native vessel and graft were illuminated with an NIR light source and fluorescent images were visualized live. In this study, the fluorescence was continuous, both in the graft and in the carotid, confirming an uninterrupted flow of blood. If there had been any block or if the anastomosis was defective, there would have been a disruption in the flow or a leak of the dye would have been clearly visible in the fluorescence.

Concurrent Doppler ultrasound measurements were used to assess the flow of blood through the graft and the carotid artery. When vascular clamps were applied to the bypass graft, fluorescence was not observed beyond the clamp, suggesting the interruption of flow. These findings were confirmed by Doppler ultrasound, which showed a parallel decrease in blood flow after the graft was occluded.

The ICG fluorescence intensity was found to decrease with time. After 7 min, there was no detectable fluorescence in both the graft and the carotid, indicating the hepatic clearance of ICG, as expected[13]. This clearance allowed for fluorescent images to be recorded following repeated injections of ICG. Therefore, all fluorescent imaging should be performed within 7 min of the injection of ICG. The image quality was improved

by lowering the gain and optimizing the dosage of ICG in a second injection on the left side. Once the contralateral grafting was completed, ICG was injected at a lower dose. A non-uniform filling pattern of ICG dye was reflected in the graft fluorescence. This non-uniform pattern indicated that the valves in the jugular vein used for grafting might have caused turbulence and resistance to the flow. Flow in the carotid artery, however, was uninterrupted. No leaks were observed in the distal and proximal anastomosis. Doppler flow measurements performed concurrently showed a variation in signals, suggesting that the flow of blood through the graft was non-uniform, as noted by the ICG pattern observed. Forceps were applied on the bypass graft to occlude the vessels (not vessel clamps, as used previously), but fluorescence was still observed beyond the clamps, suggesting that the artery forceps might have been ineffective in occluding the flow. Doppler flow measurements also confirmed that the flow was uninterrupted, despite this attempt to occlude the vessel. Finally, angiography was performed bilaterally by injecting iohexol solution intra-arterially to confirm the blood flow on both grafts, and values were consistent with previously-obtained ICG images, as well as with flow probe measurements. The use of proper vessel clamps is an essential factor that must be considered while performing the study, as it helps to establish effective blood flow and in turn to achieve grafting success.

The *in vivo* study confirmed the effectiveness and repeatability of the use of ICG and the NAVI in evaluating the patency of arteriovenous grafts (**Figure 8**). Although not yet tested in other types of surgical interventions, the study demonstrates that the NAVI will have a broad range of applications in the surgical suite. The data visualization of blood flow and the success of grafting is effective, but improvements are required prior to clinical translation to humans. Key design parameters that impact the performance of an NIR detection system for clinical translation have been analyzed and reported in a cited review[25]. Based on that, the current NAVI has certain limitations and, if minor modifications can be made, the system can be improved and utilized for several other applications. The NIR light source currently has only five LEDs for illuminating the area of interest. This sometimes result in the non-uniform distribution of light over the surgical field. Having multiple LEDs in the light source over the area of illumination can resolve this problem. Another component is to improve quality images using a high-resolution camera that has superior detection hardware. Quantitative assessment of the blood flow has not been possible with the images, and if image analysis can be integrated to achieve this, it would significantly highlight the utility of the camera. These improvements could help overcome the specified limitations and boost the NAVI capabilities. ICG dosing also plays a critical role when using the NAVI. However, based on literature reports, repeated injections are possible, as the toxicity of ICG is minimal, and optimal dosing can be achieved to obtain quality images within two or three iterations. In summary, bilateral carotid artery grafting was successfully demonstrated in a pig model, and the flow was monitored by a NAVI fluorescence imaging system. Carotid flow measurement and carotid angiography were performed to substantiate the results obtained from the fluorescence imaging. Prototype NIR imaging systems are being developed for different applications, such as real-time image-guided surgery[29,30,31,32,33], testing surgical specimens[34], CABG procedures[27], coronary artery stenoses[1], sentinel lymph node mapping[26], etc.[35]. The NIR detection systems use ICG as the NIR dye and use either LED or laser diodes as the NIR light source. The image quality is good and can be utilized for clinical applications. However, some of the systems are larger in size, making them difficult to accommodate in an operating room given space limitations. Most importantly, they are expensive, making them an unavailable resource for all hospital organizations. The fully functional and user-friendly NAVI has been shown to detect ICG fluorescence in a desirable arteriovenous grafting procedure. The compact size and reasonable cost makes this equipment accessible to even secondary and tertiary centers and stands to impact patient outcome in a positive way. The current NAVI system is not limited to graft patency procedures and can be utilized for all other applications, including intraoperative fluorescence image-guided surgery, SLN mapping, burn assessment, and skin grafting procedures. Future directions include increasing the LEDs in the NIR light source, improving the detection capability of the camera, and performing quantitative assessments of the fluorescence. Therefore, clinical utilization is imperative.

Disclosures

The authors have nothing to disclose.

Acknowledgements

References

1. Detter, C. *et al.* Fluorescent cardiac imaging: a novel intraoperative method for quantitative assessment of myocardial perfusion during graded coronary artery stenosis. *Circulation.* **116**, 1007-1014 (2007).
2. Urbanavicius, L., Pattyn, P., de Putte, D. V., & Venskutonis, D. How to assess intestinal viability during surgery: A review of techniques. *World J Gastrointest Surg.* **3**, 59-69 (2011).
3. Mack, M. J. *et al.* Results of graft patency by immediate angiography in minimally invasive coronary artery surgery. *Ann Thorac Surg.* **68**, 383-389; discussion 389-390 (1999).
4. Lin, J. C., Fisher, D. L., Szwerc, M. F., & Magovern, J. A. Evaluation of graft patency during minimally invasive coronary artery bypass grafting with Doppler flow analysis. *Ann Thorac Surg.* **70**, 1350-1354 (2000).
5. Amin, S., Pinho-Gomes, A. C., & Taggart, D. P. Relationship of Intraoperative Transit Time Flowmetry Findings to Angiographic Graft Patency at Follow-Up. *Ann Thorac Surg.* (2016).
6. Gwozdziewicz, M. Cardiomed coronary flow meter for prevention of early occlusion in aortocoronary bypass grafting. *Biomed Pap Med Fac Univ Palacky Olomouc Czech Repub.* **148**, 59-61 (2004).
7. Succi, J. E. *et al.* Intraoperative coronary grafts flow measurement using the TTFM flowmeter: results from a domestic sample. *Rev Bras Cir Cardiovasc.* **27**, 401-404 (2012).
8. Gabriel, J., Klimach, S., Lang, P., & Hildick-Smith, D. Should computed tomography angiography supersede invasive coronary angiography for the evaluation of graft patency following coronary artery bypass graft surgery? *Interact Cardiovasc Thorac Surg.* **21**, 231-239 (2015).
9. Ughi, G. J. *et al.* Clinical Characterization of Coronary Atherosclerosis With Dual-Modality OCT and Near-Infrared Autofluorescence Imaging. *JACC Cardiovasc Imaging.* (2016).

10. Takami, Y., & Masumoto, H. Transit-time flow measurement cannot detect wrong anastomosis of an internal thoracic artery with the cardiac vein in coronary artery surgery. *J Thorac Cardiovasc Surg.* **128**, 629-631 (2004).
11. Hope-Ross, M. *et al.* Adverse reactions due to indocyanine green. *Ophthalmology.* **101**, 529-533 (1994).
12. Alander, J. T. *et al.* A review of indocyanine green fluorescent imaging in surgery. *Int J Biomed Imaging.* **2012**, 940585 (2012).
13. Cherrick, G. R., Stein, S. W., Leevy, C. M., & Davidson, C. S. Indocyanine green: observations on its physical properties, plasma decay, and hepatic extraction. *J Clin Invest.* **39**, 592-600 (1960).
14. Sander, M. *et al.* Peri-operative plasma disappearance rate of indocyanine green after coronary artery bypass surgery. *Cardiovasc J Afr.* **18**, 375-379 (2007).
15. Takahashi, M., Ishikawa, T., Higashidani, K., & Katoh, H. SPY: an innovative intra-operative imaging system to evaluate graft patency during off-pump coronary artery bypass grafting. *Interact Cardiovasc Thorac Surg.* **3**, 479-483 (2004).
16. Sevick-Muraca, E. M., Kwon, S., & Rasmussen, J. C. Emerging lymphatic imaging technologies for mouse and man. *J Clin Invest.* **124**, 905-914 (2014).
17. Chong, C. *et al.* In vivo visualization and quantification of collecting lymphatic vessel contractility using near-infrared imaging. *Sci Rep.* **6**, 22930 (2016).
18. Unno, N. *et al.* Preliminary experience with a novel fluorescence lymphography using indocyanine green in patients with secondary lymphedema. *J Vasc Surg.* **45**, 1016-1021 (2007).
19. Fujiwara, M., Mizukami, T., Suzuki, A., & Fukamizu, H. Sentinel lymph node detection in skin cancer patients using real-time fluorescence navigation with indocyanine green: preliminary experience. *J Plast Reconstr Aesthet Surg.* **62**, e373-378 (2009).
20. Zarrinpar, A. *et al.* Intraoperative Laparoscopic Near-Infrared Fluorescence Cholangiography to Facilitate Anatomical Identification: When to Give Indocyanine Green and How Much. *Surg Innov.* (2016).
21. Kaiser, M., Yafi, A., Cinat, M., Choi, B., & Durkin, A. J. Noninvasive assessment of burn wound severity using optical technology: a review of current and future modalities. *Burns.* **37**, 377-386 (2011).
22. Hardesty, D. A., Thind, H., Zabramski, J. M., Spetzler, R. F., & Nakaji, P. Safety, efficacy, and cost of intraoperative indocyanine green angiography compared to intraoperative catheter angiography in cerebral aneurysm surgery. *J Clin Neurosci.* **21**, 1377-1382 (2014).
23. Kamp, M. A. *et al.* Microscope-integrated quantitative analysis of intraoperative indocyanine green fluorescence angiography for blood flow assessment: first experience in 30 patients. *Neurosurgery.* **70**, 65-73; discussion 73-64 (2012).
24. Degett, T. H., Andersen, H. S., & Gogenur, I. Indocyanine green fluorescence angiography for intraoperative assessment of gastrointestinal anastomotic perfusion: a systematic review of clinical trials. *Langenbecks Arch Surg.* (2016).
25. Gioux, S., Choi, H. S., & Frangioni, J. V. Image-guided surgery using invisible near-infrared light: fundamentals of clinical translation. *Mol Imaging.* **9**, 237-255 (2010).
26. Troyan, S. *et al.* The FLARE Intraoperative Near-Infrared Fluorescence Imaging System: A First-in-Human Clinical Trial in Breast cancer sentinel lymph node mapping. *Annal Surg Oncol.* **16**, 2943 (2009).
27. Detter, C. *et al.* Near-infrared fluorescence coronary angiography: a new noninvasive technology for intraoperative graft patency control. *Heart Surg Forum.* **5**, 364-369 (2002).
28. Tanaka, E. *et al.* Real-time assessment of cardiac perfusion, coronary angiography, and acute intravascular thrombi using dual-channel near-infrared fluorescence imaging. *J Thorac Cardiovasc Surg.* **138**, 133-140 (2009).
29. Liu, Y. *et al.* Hands-free, wireless goggles for near-infrared fluorescence and real-time image-guided surgery. *Surgery.* **149**, 689-698 (2011).
30. Wang, X., Bhaumik, S., Li, Q., Staudinger, V. P., & Yazdanfar, S. Compact instrument for fluorescence image-guided surgery. *J Biomed Opt.* **15**, 020509 (2010).
31. Gray, D. C. *et al.* Dual-mode laparoscopic fluorescence imag-guided surgery using a single camera. *Biomed Opt Exp.* **3**, 1880-1890 (2012).
32. Chen, Z., Zhu, N., Pacheco, S., Wang, X., Liang, R. Single camera imaging system for color and near-infrad fluorescence image guided surgery. *Biomed Opt Exp.* **5**, 279197 (2014).
33. De Grand, A., Frangioni, J. V. An operational nearinfra fluorescence imaging system prototype for large animal surgery. *Technol Cancer Res Treat .* **2**, 10 (2003).
34. Kakareka, J. W. *et al.* A Portable Fluorescence Camera for Testing Surgical Specimens in the Operating Room: Description and Early Evaluation. *Mol Imaging Biol.* **13**, 862-867 (2011).
35. Vahrmeijer, A. L. *et al.* Image-guided cancer surgery using near-infrared fluorescence. *Nat Rev Clin Oncol.* **10**, 507-518 (2013).